***JKPK (JURNAL KIMIA DAN PENDIDIKAN KIMIA)**, Vol. 10, No. 2, 2025* *pp. 295-308*
Chemistry Education Study Program, Universitas Sebelas Maret *ISSN 2503-4146*
https://jurnal.uns.ac.id/jkpk *ISSN 2503-4154 (online)*

IMPROVING ELECTROCHEMICAL SENSOR PERFORMANCE FOR DETECTION OF 3-MCPD BASED ON MOLECULARY IMPRINTED POLYMER-ND_2O_3-GRAPHENE

Febi Indah Fajarwati[1]*, Ganjar Fadillah[1], and Rahmat Hidayat[2]

[1]Department of Chemistry, Faculty of Mathematics and Natural Sciences, Universitas Islam Indonesia, Yogyakarta, Indonesia
[2]Department of Applied Chemistry, Politeknik Negeri Lampung, Lampung, Indonesia

ARTICLE INFO

Keywords:
Palm oil;
3-MCPD;
Electrochemical sensor;
MIPs-Nd_2O_3-Graphene.

Article History:
Received: 2025-07-16
Accepted: 2025-08-20
Published: 2025-08-31
doi:10.20961/jkpk.v10i2.106233

ABSTRACT

Palm oil is one of the raw materials for the food industry that has a large strategic value, in the refining and deodorization process it can produce 3-monochloropropane-1,2-diol (3-MCPDs) compounds which are carcinogenic. Therefore, a detection method that has high selectivity and sensitivity is needed. In this study, an electrochemical sensor based on Molecularly imprinted polymers (MIPs) was developed which was combined with Neodium oxide graphene (Nd_2O_3-Gr) material. The characterization methods used, such as Fourier Transform Infra-Red (FTIR), X-ray diffraction (XRD), and Scanning Electron Microscopy (SEM), provided evidence supporting the successful assembly and positive arrangement of MIPs-Nd_2O_3/G composites. Sensor performance tests were studied using DPV and voltammetry techniques. Modification of the MIPs-Nd_2O_3-Graphene sensor greatly improved the detection capability of 3-MCPD compounds, with excellent linearity (R^2 = 0.9932). In low-concentration detection analysis, pH significantly influences 3-MCPD detection, so the MIPs-Nd_2O_3- Graphene sensor can be used to develop sensors with good selectivity for food product control.

**Corresponding Author*: *febi.indah@uii.ac.id*
How to cite: F. I. Fajarwati, G. Fadillah, and R. Hidayat, "Improving electrochemical sensor performance for detection of 3-MCPD based on moleculary imprinted polymer-Nd_2O_3-Graphene," *Jurnal Kimia dan Pendidikan Kimia (JKPK)*, vol. 10, no. 2, pp. 295-308, 2025. [Online]. Available: https://doi.org/10.20961/jkpk.v10i2.106233

INTRODUCTION

Palm oil (*Elaeis guineensis*) is a strategic commodity that significantly contributes to the Indonesian economy. It serves as a source of foreign exchange and as a raw material for various food and non-food products. Crude palm oil (CPO) is widely used in the food industry, primarily as cooking oil, margarine, shortening, and as a raw material for processed foods. Palm oil's primary advantages lie in its high oxidative stability and high saturated fatty acid content, which support its industrial applications [1]-[4]. However, during the refining, deodorization, and fractionation of palm oil, hazardous process contaminants can be formed such as 3- and 2-monochloropropane-1,2-diol (MCPD), glycidol, and esters that are dangerous and carcinogenic [5], [6]. In recent years, 3-MCPD have been found in processed edible oils in relatively high concentration [5].

Analytical methods for determining MCPD and glycidol in processed palm oil

have been developed, including High Pressure Liquid Chromatography (HPLC) [7], Gas Chromatography (GC) [8], and HPLC-Mass Spectrometry (HPLC-MS) [9]. However, these methods are considered to still have limitations, especially for field analysis because they require complex pretreatment processes [6], [10], [11], [12]. Therefore, finding alternative analytical methods for detection of 3-MCPD is still required.

Developing electrochemical sensors presents a promising alternative approach. These sensors are easy to use, provide rapid analysis, exhibit high sensitivity, and have the potential for miniaturization for on-site applications, which offers significant advantages in terms of efficiency [13], [14]. However, the primary challenge for electrochemical sensors lies in enhancing their selectivity for target analytes when other compounds are present in the oil matrix.

Molecularly imprinted polymers (MIPs) serve as effective recognition specific compounds that address the challenge of selectivity in binding [15]-[17]. Fadillah et al. (2023) reported the MIPs on the membrane surface for enhancing selectivity separation of amino acids [18]. Their study reported that the presents MIPs could enhance the ratio selectivity in separation process. Therefore, the formation of MIPs on the electrode surface allows for increased selectivity for 3-MCPD detection through creating specific recognition sites that closely match the structure of the target molecule, which allows for the precise and selective attachment to 3-MCPD. Even though the MIPs can improve the sensor selectivity, for application as a sensor electrode, electrode performance is assessed not only by selectivity but also by sensitivity. Thus, combination with conductive materials such as carbon based materials and metal oxide are required. Integration of carbon-based materials such as graphene and rare-earth metal semiconductors as conductive materials can improve charge transfer performance and enlarge the electric current response, thanks to their high surface area [19].

Although the development of MIPs for 3-MCPD detection has been widely explored [10], [20], [21], [22], the formation of MIPs on the surface of Neodium oxide-graphene (Nd_2O_3-Gr) material has never been studied. The addition of Nd_2O_3 in the composite system can provide a synergistic effect by increasing electrocatalytic activity, decreasing charge transfer resistance, and increasing sensor stability [23]. Therefore, this research is focused on the development and improvement of the performance of MIP/Nd_2O_3–Gr-based electrochemical sensors for detecting 3-MCPD in palm oil products. This work aspires to support quality control and ensure food safety within the palm oil industry [12].

METHODS

1. Materials

The chemicals used including $NdCl_3.6H_2O$, 3-MCPD >98%, 2-MCPD >98%, pH buffers (4, 7, 10); acrylamide acid (AA), Ethylene glycol dimethacrylate (EGDMA), 1,2-propanediol, methanol were purchased from Merck in pro-analytical grade without further purification.

2. Synthesis MIP/Nd_2O_3-Gr/SPE

The composite of Nd_2O_3 was prepared following our previous study reported [20]. While for preparation of MIP printing, 10 mg/mL of Nd_2O_3-Gr in ethanol was prepared and then dropped 10 μL on the SPE surface. After that, the prepared electrode was dried over night at room temperature. Then, MIP/Nd_2O_3-Gr/SPE was prepared by electropolymerization process with acrylamide acid as monomer and 3-MCPD as template molecule with the ratio mol 1:2. The polymerization process was carried out for 10 cycles by cyclic voltammetry (CV) at potential range -0.8 V to +1.2 V with scan rate of 0.1 V/s in buffer solution pH 4.0. After polymerization was completed, the 3-MCPD was extracted from the polymer structure by immersing the electrode in methanol solution under stirred process for 5 min. Figure 1 shows the illustration of electrode preparation

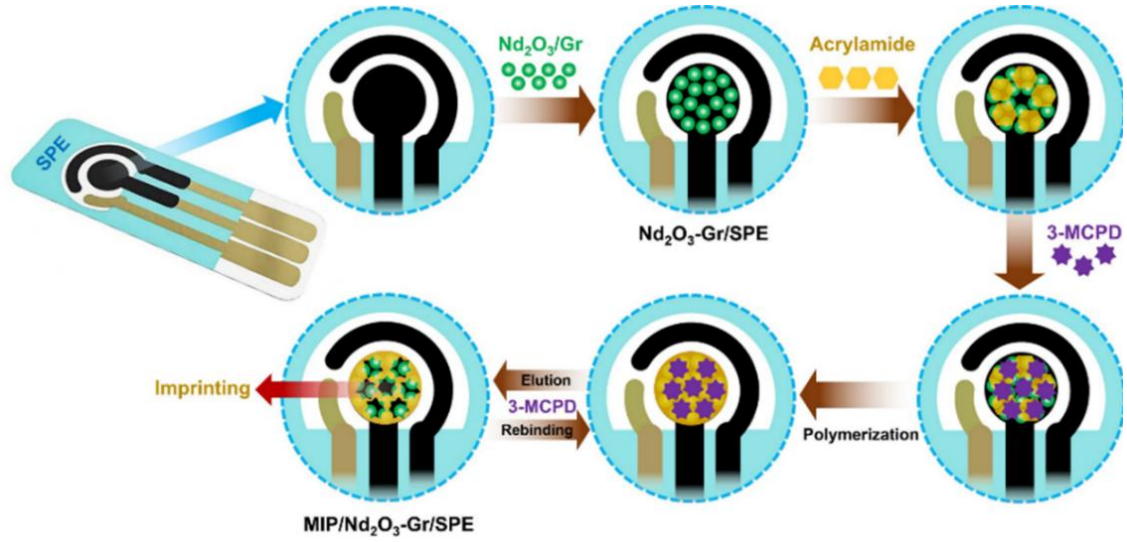

Figure 1. Illistration of MIP/Nd2O3-GR/SPE

3. Characterization

The synthesized materials were characterized using FTIR spectrophotometer (Perkin Elmer Spectrum Two System L160000A) for observing the functional groups, XRD spectrophotometer (Bruker D2 Phaser) to determine diffraction pattern and crystalline parameter, then SEM (Phenom Desktop ProXL) for imaging the morphology and composite structure. All characterization provides properties and structure of MIP/Nd_2O_3-Gr/SPE.

4. Electrochemical Studies

Electrochemical performance test of MIP/Nd_2O_3-Gr/SPE was studied by differential pulse voltammetry (DPV) under optimum conditions with three electrode systems (MIP/Nd_2O_3-Gr/SPE as working electrode, Ag/AgCl as reference electrode, and Pt wire as counter electrode). Quantitative of 3-MCPD was determined by DPV technique at potential range -0.8 V to +1.2 V with scan rate of 0.1 V/s.

RESULT AND DISCUSSION

1. Preparation of MIP/Nd_2O_3-Gr/SPE

The surface morphology characterization of the MIP/Nd_2O_3–Graphene composite was carried out using Scanning Electron Microscopy (SEM) as shown in Figure 2(a). The observation results showed a morphology in the form of thin sheets that were unevenly dispersed, which indicated the presence of a layered graphene structure. Between the graphene layers, granular particles of nano to micron size were visible, which were suspected to be Nd_2O_3 particles distributed on the graphene surface. This porous and inhomogeneous surface structure is advantageous for sensor applications because it can increase the active surface area and facilitate the adsorption process of target molecules and charge transfer [24], [25].

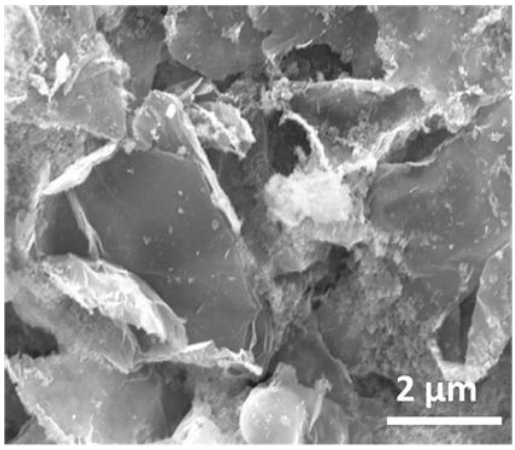

a.

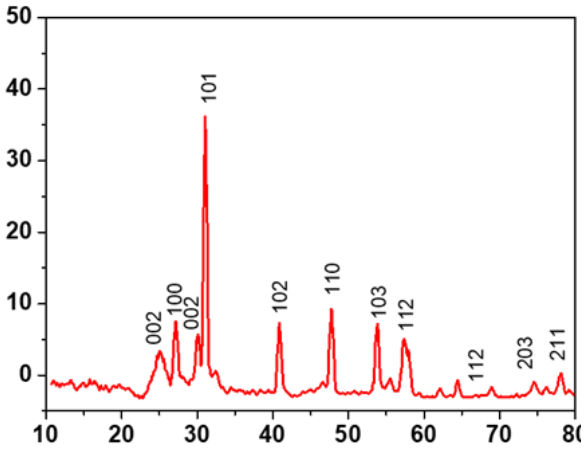

b.

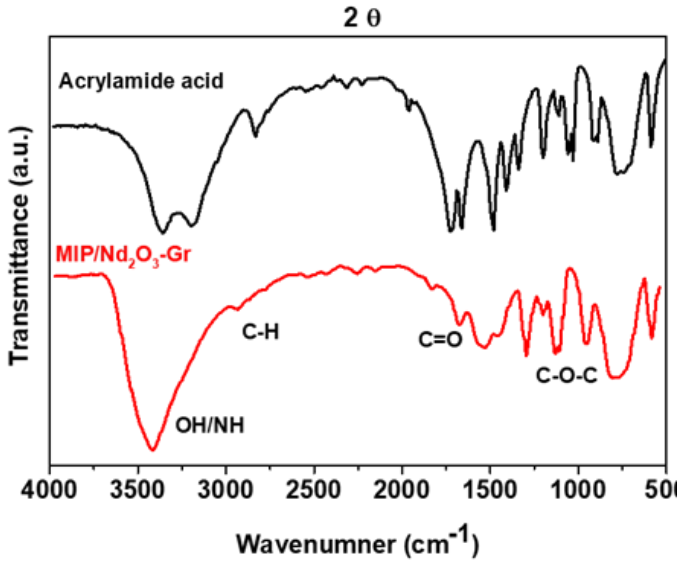

c.

Figure 2. (a) surface morphology of (b) diffractogram, and (c) IR spectrum of MIP/Nd_2O_3–Gr.

Furthermore, crystallinity characterization was performed using X-Ray Diffraction (XRD) as shown in Figure 2(b). The XRD pattern of the MIP/Nd_2O_3–Gr composite exhibits several sharp and intense diffraction peaks, confirming the crystalline nature of the material. The dominant peaks observed at around 29°, 33°, 47°, 54°, and 58° representing difraction planes of (002), (101), (110), (103), and (112) of hexagonal Nd_2O_3, in agreement with JCPDS Card No. 00-043-1023 [26]. A weaker diffraction signal near 25° also corresponds to the (002) plane of graphitic carbon, indicating the presence of graphene within the composite [27]. The relatively narrow widths of the Nd_2O_3 peaks suggest the formation of nanosized crystallites, while the absence of additional impurity peaks highlights the high purity of the synthesized material. These combined observations confirm the successful incorporation of crystalline Nd_2O_3 into the graphene-supported molecularly imprinted polymer matrix, forming a well-defined hybrid composite structure. Moreover, higher crystallinity of Nd_2O_3 improves the structural stability of the composite while supporting more efficient charge transfer through reduced recombination [28], whereas graphene remains the primary pathway for electrical conductivity [29].

The FTIR spectrum of the MIP/Nd_2O_3–Gr composite (Figure 2(c)) shows several characteristic absorption bands that confirm the successful integration of neodymium oxide into the polymer–graphene matrix. A broad band around 3400 cm^{-1} corresponds to O–H stretching vibrations, indicating the presence of surface hydroxyl groups and adsorbed water, while the peak near 1630 cm^{-1} is attributed to C=O stretching from residual carboxyl functionalities. The band in the region of 1400–1500 cm^{-1} reflects C=C skeletal vibrations of the graphene framework, and the absorption near 1100–1000 cm^{-1} corresponds to C–O stretching of epoxy or alkoxy groups, confirming oxygen-containing functional groups remain in the structure [26]. Importantly, the strong absorption observed below 600 cm^{-1} is assigned to Nd–O vibrations, providing direct evidence of the incorporation of neodymium oxide into the composite [30]. These features collectively demonstrate the coexistence of graphene functional groups with metal–oxygen bonds, validating the successful formation of the MIP/Nd_2O_3–Gr composite.

The characterization results collectively highlight how the structural features of the MIP/Nd_2O_3–Gr composite support its intended electrochemical application in 3-MCPD detection. The FTIR spectra confirm the presence of functional groups and metal–oxygen bonds that facilitate selective binding interactions between the imprinted polymer and the target analyte. The XRD analysis demonstrates high crystallinity of Nd_2O_3, which contributes to structural stability and minimizes defect-mediated charge trapping, while the incorporation of graphene ensures a continuous conductive pathway for efficient electron transfer. The surface roughness from morphological picture provide evidence the accessibility of active sites. Simultaneously, these properties create a synergistic balance of stability and molecular

recognition capability, thereby improving the sensitivity and selectivity of the composite electrode toward 3-MCPD detection.

X-ray diffraction Figure 2(b) displays sharp, intense reflections at ~29°, 33°, 47°, 54°, and 58°, indexed to the (002), (101), (110), (103), and (112) planes of hexagonal Nd_2O_3 (JCPDS 00-043-1023), confirming high crystallinity. A weak feature near 25° corresponds to the (002) reflection of graphitic carbon, evidencing graphene within the composite, while the absence of extraneous peaks indicates phase purity and nanoscale crystallites inferred from peak narrowing. Complementary FTIR spectra (Figure 2c) exhibit O–H stretching (~3400 cm^{-1}), C=O stretching (~1630 cm^{-1}), graphene C=C skeletal modes (1400–1500 cm^{-1}), and C–O vibrations (1000–1100 cm^{-1}), alongside strong Nd–O bands below 600 cm^{-1} that directly verify neodymium oxide incorporation. Spectroscopic signatures therefore validate the coexistence of graphene functional groups and metal–oxygen bonds within a polymer-imprinted architecture, consistent with successful assembly of the MIP/Nd_2O_3–Gr hybrid. Crystalline Nd_2O_3 is expected to enhance structural stability and curtail defect-mediated charge trapping, whereas graphene furnishes a continuous, low-resistance pathway for electron transport and interfacial charge exchange. Morphological roughness observed in the micrographs further suggests improved accessibility of imprinted binding cavities and electroactive sites. Collectively, the diffraction and vibrational evidence rationalize the high sensitivity and selectivity achieved for 3-MCPD detection through the synergistic coupling of MIP-mediated molecular recognition with Nd_2O_3-assisted electrocatalysis and graphene-enabled conductivity.

2. Electrochemical Performance Test

The performance of the MIP/Nd_2O_3–Gr/SPE-based electrochemical sensor against the 3-MCPD analyte was evaluated by measuring the analyte using the DPV technique over a potential range of -0.8 V to +1.2 V. First, the linearity of the developed sensor, operated in a single-electrode configuration, was investigated, as shown in Figure 3(a). The figure shows the relationship between the oxidation peak current (Ip) and the concentration of 3-MCPD. The results demonstrate a linear relationship between the peak current intensity and the concentration of 3-MCPD within a specific range, as indicated by the regression equation Ip = 0.096 [MCPD] + 1.3368, with a coefficient of determination R^2 = 0.9932 for MIP/Nd_2O_3–Gr/SPE. The R^2 value of nearly 1 indicates that the sensor exhibits excellent linearity, making it a reliable choice for quantifying analytes. The increase in peak current with increasing analyte concentration indicates that the sensor material can effectively bind and recognize 3-MCPD, a finding strengthened by the role of MIP as a selective recognition layer. Although Nd_2O_3–Gr/SPE shows good linearity values, the current response at the same concentration is lower compared to MIP/Nd_2O_3–Gr/SPE. Based on the calibration curve, the LOD and LOQ were calculated as 3σ/S and 10σ/S, respectively. This is also in line with Figure

3(b), which shows that the LOD value of MIP/Nd_2O_3–Gr/SPE is lower than that of Nd_2O_3–Gr/SPE, indicating that the sensor is more sensitive. Based on international regulations, the maximum limit for 3-MCPD contamination varies depending on the product type and the target consumer group. The European Commission, through Regulation (EU) No. 1881/2006, which has been updated to Regulation (EU) 2020/1322, sets the limit for 3-MCPD esters in oils and fats at 2,500 µg/kg for general consumption, while for baby food products, the limit is set much stricter, at 750 µg/kg. In Indonesia, a specific maximum limit reference has not been explicitly stated in BPOM regulations, but mitigation research refers to general limits for vegetable oils that align with European Union provisions. In this study, the measured 3-MCPD concentration of 41.77 µM, equivalent to approximately 4,616 µg/kg, indicates a value exceeding the maximum limit applicable to various food categories, particularly for baby products with a very low threshold. However, detection techniques can still be improved with preconcentration techniques to be detected with the developed sensor. Second, sensitivity determination is performed by creating a graph of the relationship between pH and potential, as shown in Figure 3(c).

This relationship is derived from the basic Nernstian equation, which states a linear relationship between pH and E, with a slope value indicating sensitivity. The sensitivity is determined by testing the sensor in pH solutions in phosphate buffer solution (PBS) in the range 2-12. Observations show that the pH of the solution has a significant effect on the peak oxidation potential value. The plot results between peak potential and pH produce a linear relationship with the equation E = 0.0591 pH + 0.05 for MIP/Nd_2O_3–Gr/SPE. This compound has a hydroxyl group (–OH) and a chloromethyl group, which are hydrophilic and capable of forming hydrogen bonds at the electrode interface. The hydroxyl group can act as a proton donor or acceptor depending on the solution pH, thus influencing the redox potential through a pH-dependent protonation–deprotonation equilibrium. The linear increase in oxidation potential with increasing pH indicates the involvement of protons in the electrochemical reaction mechanism of 3-MCPD on the sensor surface. The slope value of 0.0591 V/pH is close to the Nernstian slope theory for redox reactions involving the number of electron and proton transfers in a 1:1 proportion, which is 0.0592, which strengthens the suspicion that the detection mechanism takes place through a reaction involving simultaneous charge and proton transfer. Additionally, Figure 3(d) presents a summary of the sensitivity. Based on the graph, it can be seen that the sensitivity of MIP/Nd_2O_3–Gr/SPE is higher and approaches the theoretical Nernstian slope. This indicates the synergistic role of the combination of MIP as a selective recognition layer, graphene as a conductive medium, and Nd_2O_3 as an electrocatalytic material, which together enhances the sensor's sensitivity.

Differential pulse voltammetry (−0.8 to +1.2 V) revealed a proportional increase in oxidation peak current with 3-MCPD concentration, as summarized in Figure 3(a).

Calibration of MIP/Nd_2O_3–Gr/SPE yielded Ip = 0.096[MCPD] + 1.3368 with R^2 = 0.9932, evidencing excellent linearity and reliable quantification performance. Compared with the non-imprinted Nd_2O_3–Gr/SPE, the imprinted platform delivered higher current responses at equal concentrations, consistent with selective preconcentration at MIP recognition sites. Limits of detection and quantification were estimated via 3σ/S and 10σ/S, respectively, with MIP/Nd_2O_3–Gr/SPE achieving a lower LOD (Figure 3b), indicative of superior sensitivity. Regulatory context underscores analytical relevance: EU provisions (Reg. (EU) 2020/1322) cap 3-MCPD esters in oils/fats at 2,500 µg/kg and in infant foods at 750 µg/kg, whereas the studied sample (41.77 µM ≈ 4,616 µg/kg) exceeds these thresholds, warranting sensitive monitoring and potential preconcentration. pH-dependent analysis showed a linear potential shift described by E = 0.0591 pH + 0.05 (Figure 3c), approximating the Nernstian slope (0.0592 V/pH) for a 1:1 electron–proton coupled process at the interface. Altogether, the near-Nernstian behavior and enhanced calibration metrics (Figure 3d) reflect a synergistic contribution of MIP-mediated recognition, graphene-facilitated charge transfer, and Nd_2O_3 electrocatalysis to the high sensitivity and selectivity of the sensor.

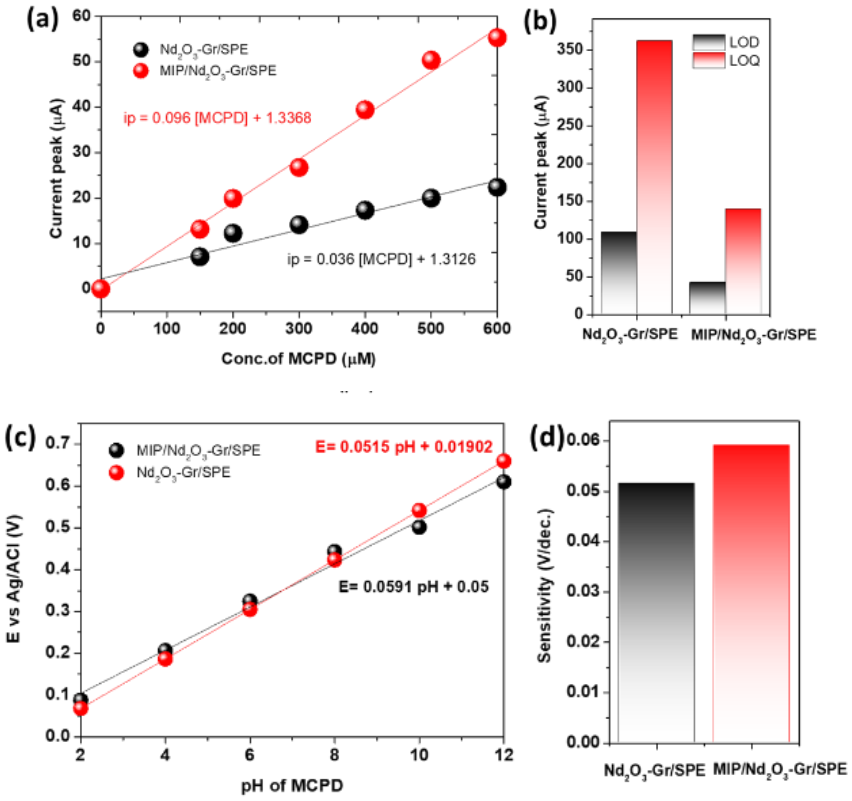

Figure 3.(a) linearity test of 3-MCPD, (b) LOD value, (c) relationship between pH vs E, and (d) sensitivity results.

The selectivity of the MIP/Nd_2O_3–Graphene-based sensor toward 3-MCPD was tested by comparing the peak current responses to several analog compounds,

namely 1,2-propanediol and 2-MCPD, as shown in Figure 4(a). The voltammogram results show that only 3-MCPD produces a significant peak oxidation current signal, appearing at a potential of approximately 0.21 V (vs. Ag/AgCl) with a peak current intensity of approximately 79 µA. In contrast, analog compounds such as 1,2-propanediol and 2-MCPD exhibit significantly lower peak currents, whereas lactic acid does not exhibit a substantial electrochemical response within the same potential range.

The fact that 1,2-propanediol (which lacks a chloride group) and 2-MCPD (a structural isomer of 3-MCPD) produced much smaller signals than 3-MCPD indicates that the recognition of the target molecule by the Molecularly Imprinted Polymer (MIP) layer is particular to the 3-MCPD molecular configuration. This demonstrates the success of the imprinting technique in producing a recognition cavity that matches the size, shape, and distribution of functional groups. Furthermore, the absence of a significant signal from lactic acid, which has both hydroxyl and carboxyl groups, confirms that the electrochemical interaction is not solely due to the presence of the hydroxyl group but also involves recognition of the chloride group and the overall structure of the 3-MCPD molecule. In the printing stage, 3-MCPD serves as a template that forms a recognition cavity with complementarity in the shape and location of functional groups: (i) the vicinal diol pair C1–C2 (–CHOH–CH_2OH) provides two hydrogen bond donors/acceptors arranged close together for bidentate trapping, and (ii) the –CH_2Cl substituent at C3 provides a specific steric/polar fit at the tip of the cavity. After removing the template, this site only “fits” for molecules with the distance between the –OH groups and the volume of the chloromethyl end as in 3-MCPD [21], [31]. In 2-MCPD, the diol is at the 1,3 position (non-vicinal), so the geometry is no longer suitable for bidentate trapping; as a result, the bond energy is weaker and the pre-concentration at the surface decreases. Meanwhile, 1,2-propanediol does not have –CH_2Cl, so it loses the additional interaction (polar/halogen-acceptor) and does not fulfill the steric features of the cavity.

Figure 4(b), which displays a histogram of the peak current comparison, further emphasizes that 3-MCPD produces the highest peak current signal among the other compounds tested, with a significant difference exceeding the measurement error limit (error bar). These results demonstrate that the sensor has high selectivity for 3-MCPD, even in the presence of structurally similar interfering compounds. Overall, these results demonstrate that the MIP/Nd_2O_3–Graphene composite is capable of selectively recognizing and detecting 3-MCPD among other analogous compounds, supporting the potential application of this sensor for the selective analysis of 3-MCPD in complex samples such as oil or food products. This emphasizes the synergistic role between molecular imprinting (MIP) and Nd_2O_3–Graphene functional materials in the developed electrochemical sensor system.

Voltammetric analyses indicate that 3-MCPD exhibits a distinctive oxidation peak at ~0.21 V with a peak current near 79 µA, whereas 2-MCPD, 1,2-propanediol, and

lactic acid yield attenuated or negligible responses. The inter-analyte differences—visualized in Figure 4(a–b)—exceed experimental error bounds, supporting statistically meaningful selectivity. This pattern accords with an imprinting-mediated recognition mechanism in which MIP cavities complement the vicinal diol (C1–C2) and the chloromethyl substituent at C3 of 3-MCPD. In 2-MCPD, the non-vicinal 1,3-diol geometry disrupts bidentate trapping and diminishes surface preconcentration, while 1,2-propanediol lacks the $–CH_2Cl$ group needed for polar/halogen-acceptor interactions and steric complementarity. Lactic acid's minimal response further indicates that hydroxyl functionality alone is insufficient, implicating cooperative recognition of both diol topology and chloromethyl volume. The Nd_2O_3–Graphene scaffold augments electron transfer and adsorption, amplifying the imprinting-driven molecular discrimination. Altogether, the MIP/Nd_2O_3–Graphene composite constitutes a robust and highly selective platform for accurate 3-MCPD quantification in complex food-oil matrices.

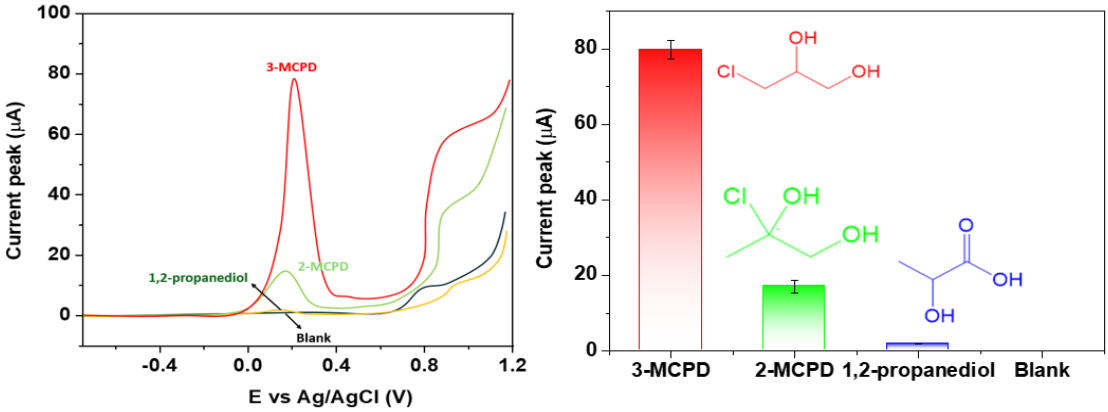

Figure 4. The voltammogram and selectivity results of the developed sensor.

CONCLUSION

MIP/Nd_2O_3–Gr-based electrochemical sensor was successfully developed and demonstrated good performance for the detection of 3-MCPD. Characterization demonstrated the formation of a material with a porous structure, crystalline Nd_2O_3 content, and active functional groups. This sensor exhibited a linear response to 3-MCPD concentration (R^2 = 0.9932), with a low detection limit and high sensitivity, which was influenced by pH. Selectivity tests demonstrated that the sensor was able to distinguish 3-MCPD from analogous compounds, thanks to the specific recognition of the MIP layer. Overall, the MIP/Nd_2O_3–Gr composite has potential as a sensitive and selective electrochemical sensor for analyzing 3-MCPD in food products

ACKNOWLEDGEMENT

This research was supported by funding from Ministry of Higher Education,

Science and Technology of Indonesia Republic (022/DirDPPM/70/DPPM/PFRKEMDIKTISAINTEK/VI/2025). We are deeply grateful for their financial assistance, which made this study possible for contributing valuable insights to the field.

REFERENCES

[1] H. Rahman, J. P. Sitompul, and S. Tjokrodiningrat, "The composition of fatty acids in several vegetable oils from Indonesia," *Biodiversitas Journal of Biological Diversity*, vol. 23, no. 4, pp. 2167–2176, 2022, doi: https://doi.org/10.13057/biodiv/d230452

[2] Z. Xu, Z. Ye, Y. Li, J. Li, and Y. Liu, "Comparative study of the oxidation stability of high oleic oils and palm oil during thermal treatment," *Journal of Oleo Science*, vol. 69, no. 6, pp. 573–584, 2020, doi: https://doi.org/10.5650/jos.ess19307

[3] R. Jędrkiewicz, M. Kupska, A. Głowacz, J. Gromadzka, and J. Namieśnik, "3-MCPD: A worldwide problem of food chemistry," *Critical Reviews in Food Science and Nutrition*, vol. 56, no. 14, pp. 2268–2277, 2016, doi: https://doi.org/10.1080/10408398.2013.829414

[4] E. Mela and D. S. Bintang, "Virgin coconut oil (VCO): production, advantages, and potential utilization in various food products," *Jurnal Penelitian dan Pengembangan Pertanian*, vol. 40, no. 2, pp. 103–110, 2021, doi: https://doi.org/10.21082/jp3.v40n2.2021.p103-110

[5] R. G. Tivanello *et al.*, "Mitigation studies based on the contribution of chlorides and acids to the formation of 3-MCPD, 2-MCPD, and glycidyl esters in palm oil," *ACS Food Science & Technology*, vol. 1, no. 7, pp. 1190–1197, 2021, doi: https://doi.org/10.1021/acsfoodscitech.1c00084

[6] S. S. Syed Putra *et al.*, "3-Monochloropropane-1,2-diol (3-MCPD): A review on properties, occurrence, mechanism of formation, toxicity, analytical approach and mitigation strategy," *Journal of Food Measurement and Characterization*, vol. 17, no. 4, pp. 3592–3615, 2023, doi: https://doi.org/10.1007/s11694-023-01883-y

[7] H. Zhou, Q. Jin, X. Wang, and X. Xu, "Direct measurement of 3-chloropropane-1,2-diol fatty acid esters in oils and fats by HPLC method," *Food Control*, vol. 36, no. 1, pp. 111–118, 2014, doi: https://doi.org/10.1016/j.foodcont.2013.07.041

[8] P. Ioime, E. Piva, M. Pozzebon, and J. P. Pascali, "Automated sample preparation and analysis by gas chromatography tandem mass spectrometry (GC–MS/MS) for the determination of 3- and 2-monochloropropanediol (MCPD) esters and glycidyl esters in edible oils," *Journal of Chromatography A*, vol. 1650, 462253, 2021, doi: https://doi.org/10.1016/j.chroma.2021.462253

[9] E. Moravcová, L. Vaclavik, O. Lacina, V. Hrbek, K. Riddellová, and J. Hajšlová, "Novel approaches to analysis of 3-chloropropane-1,2-diol esters in vegetable oils," *Analytical and Bioanalytical Chemistry*, vol. 402, no. 9, pp. 2871–2883, 2012, doi:

https://doi.org/10.1007/s00216-011-5696-3

[10] Y. T. Yaman, G. Bolat, T. B. Saygın, and S. Abacı, "Molecularly imprinted label-free sensor platform for impedimetric detection of 3-monochloropropane-1,2-diol," *Sensors and Actuators B: Chemical*, vol. 328, 128986, 2021, doi: https://doi.org/10.1016/j.snb.2020.128986

[11] W. Kim *et al.*, "Analysis of 3-MCPD and 1,3-DCP in various foodstuffs using GC-MS," *Toxicological Research*, vol. 31, no. 3, pp. 313–319, 2015, doi: https://doi.org/10.5487/TR.2015.31.3.313

[12] S. N. S. N. Mahiran, N. H. Abd Kadir, M. Maulidiani, T. R. T. Mohamad, N. J. Gooderham, and M. A. B. Md. Alam, "Multivariate modelling analysis for prediction of glycidyl esters and 3-monochloropropane-1,2-diol (3-MCPD) formation in periodically heated palm oil," *Heliyon*, vol. 9, no. 10, e20413, 2023, doi: https://doi.org/10.1016/j.heliyon.2023.e20413

[13] F. M. Oliveira, J. Azadmanjiri, X. Wang, M. Yu, and Z. Sofer, "Structure design and processing strategies of MXene-based materials for electromagnetic interference shielding," *Small Methods*, vol. 7, no. 7, 2300112, 2023, doi: https://doi.org/10.1002/smtd.202300112

[14] E. Buffon and N. R. Stradiotto, "Disposable p-coumaric acid sensor containing reduced graphene oxide, nickel nanoparticles and biodegradable molecularly imprinted polymer for fruit peel analysis," *Journal of Food Composition and Analysis*, vol. 118, 105186, 2023, doi: https://doi.org/10.1016/j.jfca.2023.105186

[15] M. B. Regasa, T. R. Soreta, O. E. Femi, P. C. Ramamurthy, and S. Kumar, "Molecularly imprinted polyaniline molecular receptor–based chemical sensor for the electrochemical determination of melamine," *Journal of Molecular Recognition*, vol. 33, no. 7, e2836, 2020, doi: https://doi.org/10.1002/jmr.2836

[16] X. Bai, B. Zhang, M. Liu, X. Hu, G. Fang, and S. Wang, "Molecularly imprinted electrochemical sensor based on polypyrrole/dopamine@graphene incorporated with surface molecularly imprinted polymers thin film for recognition of olaquindox," *Bioelectrochemistry*, vol. 132, 107398, 2020, doi: https://doi.org/10.1016/j.bioelechem.2019.107398

[17] H. da Silva, J. G. Pacheco, J. M. Magalhães, S. Viswanathan, and C. Delerue-Matos, "MIP-graphene-modified glassy carbon electrode for the determination of trimethoprim," *Biosensors and Bioelectronics*, vol. 52, pp. 56–61, 2014, doi: https://doi.org/10.1016/j.bios.2013.08.035

[18] G. Fadillah, K. Toda, and S.-I. Ohira, "One-stage chiral enrichment process by continuous flow electrodialysis with molecularly imprinted membrane," *Separation and Purification Technology*, vol. 305, 122492, 2023, doi: https://doi.org/10.1016/j.seppur.2022.122492

[19] T. A. Saleh and G. Fadillah, "Recent trends in the design of chemical sensors based on graphene–metal oxide nanocomposites for the analysis of toxic species and biomolecules," *TrAC Trends in Analytical Chemistry*, vol. 120, 115660, 2019, doi: https://doi.org/10.1016/j.trac.2019.115660

[20] W. Cheng, Q. Zhang, D. Wu, Y. Yang, Y. Zhang, and X. Tang, "A facile electrochemical method for rapid determination of 3-chloropropane-1,2-diol in soy sauce based on nanoporous gold capped with molecularly imprinted polymer," *Food Control*, vol. 134, 108750, 2022, doi: https://doi.org/10.1016/j.foodcont.2021.108750

[21] I. R. Banurea, A. R. Sanjaya, N. M. Nizardo, and T. A. Ivandini, "Molecularly imprinted polymer of p-amino thiophenol for a 3-monochloropropane-1,2-diol impedance-based sensor," *Materials Chemistry and Physics*, vol. 301, 127613, 2023, doi: https://doi.org/10.1016/j.matchemphys.2023.127613

[22] K. M. Goh, Y. H. Wong, C. P. Tan, and K. L. Nyam, "A summary of 2-, 3-MCPD esters and glycidyl ester occurrence during frying and baking processes," *Current Research in Food Science*, vol. 4, pp. 460–469, 2021, doi: https://doi.org/10.1016/j.crfs.2021.07.002

[23] R. Hidayat, G. Fadillah, F. I. Fajarwati, A. D. N. Ramdani, and Q. A. Hanif, "Highly sensitive electrochemical sensor based Nd2O3/graphene for monitoring additive compounds in palm oil product," *Materials Chemistry and Physics*, vol. 329, 130121, 2025, doi: https://doi.org/10.1016/j.matchemphys.2024.130121

[24] S. Kang *et al.*, "Highly sensitive pressure sensor based on bioinspired porous structure for real-time tactile sensing," *Advanced Electronic Materials*, vol. 2, no. 12, 1600356, 2016, doi: https://doi.org/10.1002/aelm.201600356

[25] S. Wang *et al.*, "Constructing a novel composite of molecularly imprinted polymer-coated AuNPs electrochemical sensor for the determination of 3-nitrotyrosine," *Electrochimica Acta*, vol. 259, pp. 893–902, 2018, doi: https://doi.org/10.1016/j.electacta.2017.11.033

[26] E. H. Sujiono, A. M. A. Saputra, B. D. Usman, N. Fadilah, D. Zabrian, and N. Azizah, "Coconut shell waste-derived graphene oxide composite with neodymium oxide (Nd2O3) for advanced applications," *Results in Materials*, vol. 20, 100480, 2023, doi: https://doi.org/10.1016/j.rinma.2023.100480

[27] R. Hidayat, S. Wahyuningsih, and A. H. Ramelan, "Simple synthesis of rGO (reduced graphene oxide) by thermal reduction of GO (graphene oxide)," in *IOP Conference Series: Materials Science and Engineering*, vol. 858, no. 1, 012009, 2020, doi: https://doi.org/10.1088/1757-899X/858/1/012009

[28] K. Alshammari, T. Alashgai, A. H. Alshammari, M. M. Abdelhamied, S. Alotibi, and A. Atta, "Effects of Nd2O3 nanoparticles on the structural characteristics and

dielectric properties of PVA polymeric films," *Polymers*, vol. 15, no. 20, 4084, 2023, doi: https://doi.org/10.3390/polym15204084

[29] T. Munawar *et al.*, "Rational design and electrochemical validation of reduced graphene oxide (rGO) supported CeO2–Nd2O3/rGO ternary nanocomposite as an efficient material for supercapacitor electrodes," *Journal of Applied Electrochemistry*, vol. 53, no. 9, pp. 1853–1868, 2023,

[30] R. Lok, E. Budak, and E. Yilmaz, "Structural characterization and electrical properties of Nd2O3 by sol–gel method," *Journal of Materials Science: Materials in Electronics*, vol. 31, no. 4, pp. 3111–3118, 2020, doi: https://doi.org/10.1007/s10854-020-02857-2

[31] V. H. Özyurt, G. Can, and Ü. Anık, "Development of electrochemical 3-MCPD sensor based on molecularly imprinted polymer coating on metal organic framework modified gold electrode," *Journal of Food Composition and Analysis*, vol. 138, 107004, 2025, doi: https://doi.org/10.1016/j.jfca.2024.107004